
V-LoL🤔: A Diagnostic Dataset for Visual Logical Learning

Lukas Helff^{1,2} * Wolfgang Stammer^{1,2} * Hikaru Shindo¹ Devendra Singh Dhami^{1,2}

Kristian Kersting^{1,2,3,4}

¹AI and ML Group, TU Darmstadt; ²Hessian Center for AI (hessian.AI)

³Centre for Cognitive Science, TU Darmstadt ; ⁴German Center for AI (DFKI)
{first name}.{last name}@tu-darmstadt.de

Abstract

Despite the successes of recent developments in visual AI, different shortcomings still exist; from missing exact logical reasoning, to abstract generalization abilities, to understanding complex and noisy scenes. Unfortunately, existing benchmarks, were not designed to capture more than a few of these aspects. Whereas deep learning datasets focus on visually complex data but simple visual reasoning tasks, inductive logic datasets involve complex logical learning tasks, however, lack the visual component. To address this, we propose the visual logical learning dataset, V-LoL, that seamlessly combines visual and logical challenges. Notably, we introduce the first instantiation of V-LoL, V-LoL🚂, – a visual rendition of a classic benchmark in symbolic AI, the Michalski train problem. By incorporating intricate visual scenes and flexible logical reasoning tasks within a versatile framework, V-LoL🚂 provides a platform for investigating a wide range of visual logical learning challenges. We evaluate a variety of AI systems including traditional symbolic AI, neural AI, as well as neuro-symbolic AI. Our evaluations demonstrate that even state-of-the-art AI faces difficulties in dealing with visual logical learning challenges, highlighting unique advantages and limitations specific to each methodology. Overall, V-LoL opens up new avenues for understanding and enhancing current abilities in visual logical learning for AI systems. Code and data are available at <https://sites.google.com/view/v-lol>.

1 Introduction

The ability to draw logical conclusions based on visual evidence lies at the core of human cognition. This seamless integration between vision and logical reasoning is a longstanding goal for visual AI, as researchers strive to develop artificial systems that can emulate this aspect of human intelligence. While the majority of deep learning datasets and benchmarks focus on perception challenges [34, 8, 29, 48], some do involve high-level reasoning tasks [61, 27, 24, 1, 59, 26, 60] such as scene understanding or visual question answering (VQA). However, most of these require simple reasoning abilities and, more importantly, none of these incorporate tasks that require exact logical reasoning. Conversely, classic benchmarks within inductive logic programming (ILP) [37, 38, 16] lack the visual component required for AI models to interact in our complex visual surroundings.

In this paper, we introduce the Visual Logical Learning dataset (V-LoL), a novel dataset which offers an unprecedented challenge for visual AI models. The fundamental idea of V-LoL remains to integrate the explicit logical learning tasks of classic symbolic AI benchmarks into visually complex

*equal contribution

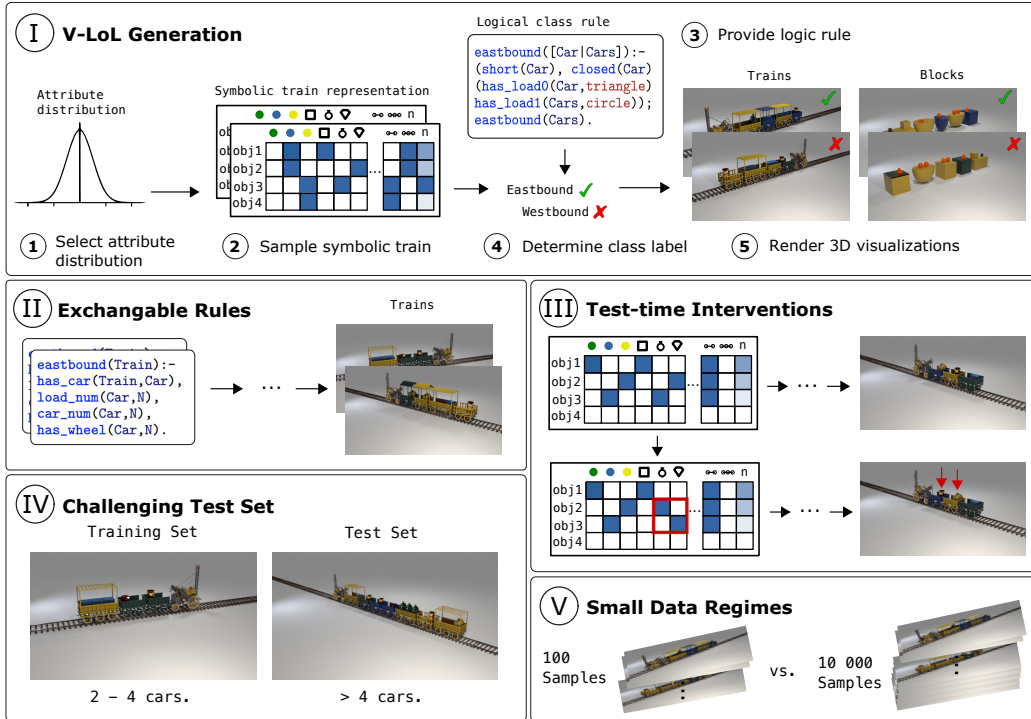


Figure 1: V-LoL: a diagnostic dataset that allows to test a variety of visual logical learning challenges. (I) The generation process of V-LoL consists of sampling symbolic train representations (*i.e.* train cars and their attributes) from a pre-defined distribution. Via a logical class rule the class affiliation of each train sample is determined and finally the 3D visual representations are rendered with different visual complexity. (II) The logic rules can easily be exchanged allowing for great versatility in data generation for specific learning challenges, *e.g.* inherent counting abilities of a model. (III) One can test the behaviour of trained models via tailored test-time interventions, *e.g.* interventions on the order of car pay loads. (IV) By increasing the number of cars in the test set one can test for abstract generalization abilities of a model, also (V) via small dataset sizes.

scenes, creating a unique visual input that retains the challenges and versatility of explicit logic. In doing so, V-LoL bridges the gap between symbolic AI challenges and contemporary deep learning datasets offering various visual logical learning tasks that pose challenges for AI models across a wide spectrum of AI research, from symbolic to neural and neuro-symbolic AI.

We present V-LoL-Trains (V-LoL), an instantiation of V-LoL that serves as an image classification dataset rendered in a CLEVR [27]-like fashion, using the symbolic representations of the Michalski train problem [37]. In contrast to the relatively straightforward visual reasoning task offered by CLEVR, V-LoL leverages the logical foundation of the Michalski train problem to establish more intricate visual logical learning problems. The V-LoL generator seamlessly integrates any provided logic rule into appealing, yet complex images (*cf.* Fig. 1 (I)), enabling precise control over the visual and logical task difficulty. The generated tasks can encompass a wide range of challenges, including object recognition, counting, interpretation of spatial arrangements, comprehension of arithmetic and logical operators, and identifying and decoding intricate, chained reasoning patterns (*cf.* Fig. 1). We use V-LoL to evaluate and compare symbolic, neural and neuro-symbolic AI revealing the benefits and shortcomings arising from different methodologies.

Overall, we make several important contributions: (i) We introduce the Visual Logical Learning dataset (V-LoL) that brings logic-based ILP benchmarks into the realm of deep learning. (ii) We present V-LoL, an initial instantiation of V-LoL that builds upon the logical foundation of the Michalski train problem and the immersive environment of CLEVR to establish a modern AI dataset that is relevant across the spectrum of AI research. (iii) The provided V-LoL generator offers great flexibility within the visual and logical components, allowing to seamlessly integrate any arbitrary logic program into a new visually complex dataset. (iv) We provide a flexible and user-friendly

Table 1: A comparison between V-LoL_{3D} and other visual reasoning datasets. We here differentiate between: 3D visualization, compositional objects (objects that consist of other objects), rich scene information (*e.g.* depth maps, pixel-wise segmentations, etc.), variable number of test objects (in comparison to training set), inclusion of programmable logic (PL), reasoning about relations, arithmetics, and analogies, and ILP problem.

Dataset	3D	Comp. Objs.	Rich Scene Information	Variable # Test Objs.	PL	Relation	Arithmetic	Analogy	ILP
VQA [1]	✓	✗	✗	✗	✗	✓	✗	✗	✗
CLEVR [27]	✓	✗	✗	(✓)	✗	✓	✓	✗	✗
CLEVR-Hans3 [53]	✓	✗	✗	(✓)	✗	✓	✗	✗	✗
PTR [24]	✓	✓	✓	✗	✗	✓	✓	✓	✗
Kandinsky [22, 23]	✗	✗	✗	(✓)	✗	✓	✓	✓	✗
RAVEN [60]	✗	✓	✗	✗	✗	✓	✓	✓	✗
V-LoL_{3D}	✓	✓	✓	✓	✓	✓	✓	✓	✓

framework, allowing for a straightforward generation of large-scale visual datasets and rich scene information. (v) By evaluating various symbolic, neural, and neuro-symbolic AI models on several V-LoL_{3D} challenges, we offer valuable insights into their visual logical learning abilities, exemplifying the value of V-LoL for investigating shortcomings and thereby helping improve AI models.

2 V-LoL: Merging Logic and Vision


V-LoL encompasses a wide range of visual logical learning datasets, specifically designed to integrate logical reasoning challenges of ILP tasks into complex visual scenes. In an ILP problem a logic rule is learned given a set of positive and negative examples and background knowledge, where the examples and knowledge are represented as logical formulae [40]. The *Michalski train problem* [37] is a classic ILP task that consists of two sets of five train examples. These trains are composed of a wide variety of properties, and labelled into two categories: *eastbound* or *westbound* (*cf.* Fig. 5 in the supplementary material (supp.)). The objective is to induce relational patterns for classifying trains based on their properties.

V-LoL-Trains (V-LoL_{3D}) is a first instantiation of V-LoL that realizes the Michalski train problem [37] in immersive visual scenes using the CLEVR [27] environment. Each V-LoL_{3D} image portrays a 3D scene with compositional objects (objects containing other objects) and is accompanied with rich scene information including depth maps, object segmentations and bounding boxes. Through the incorporation of programmable logic, V-LoL_{3D} offers significant versatility in the posed visual logical learning tasks, encompassing relational, arithmetic, and analogical reasoning. In Tab. 1 we compare V-LoL_{3D} with other visual reasoning datasets, focusing on the essential features and learning tasks of the dataset.

2.1 V-LoL_{3D} Generation

V-LoL_{3D} images are generated in two steps: first sampling a valid symbolic representation of a train and then visualizing it within a 3D scene.

Generating symbolic trains. The symbolic train representation (symbolic train) of V-LoL_{3D} are based on objects and relationships that are semantically similar to those of the prolog representation of Muggleton [39] (*cf.* Tab. 2 in supp.). Accordingly, while the trains have different attributes and associated allocations, the overall composition, number of attributes, as well as the number of corresponding allocations (groundings), remain identical. For more detailed information on the individual attributes, please refer to Fig. 2 (top). To generate symbolic trains, V-LoL_{3D} allows sampling from two different attribute distributions ((1) of Fig. 1 (top)), namely the *Michalski train* and the *random train* (*i.e.* uniform) distribution. With the *Michalski train* distribution, our dataset aims to preserve statistical coherence to the original Michalski trains [37]. To do so, we integrate the prolog train-generator from [39], which incorporates assumptions regarding the value distribution of the train attributes and follows the constraints outlined in the supplement. With the *random trains* distribution we do not impose any assumptions regarding the distribution of train attributes and only apply attribute constraints necessary for visualization (*e.g.* a short car cannot accommodate more than two payloads). Next, a symbolic train is randomly sampled from the chosen distribution



V-LoL

Car Position	Car Colour	Car Length	Car Wall	Car Roof	Car Axles	Load Num.	Load Shape
1	Yellow	Short	Full	None	2	0	Blue Box
2	Green	Long	Railing	Frame	3	1	Golden Vase
3	Grey			Flat		2	Barrel
4	Red			Bars		3	Diamond
	Blue			Peaked			Metal Pot
							Oval Vase
							None

V-LoL

Car Position	Car Colour	Car Length	Black Top	Car Shape	Black Bottom	Load Num.	Load Shape
1	Yellow	Short	True	Cube	True	0	Sphere
2	Green	Long	False	Cylinder	False	1	Pyramid
3	Grey			Hemisphere		2	Cube
4	Red			Frustum		3	Cylinder
	Blue			Hex. Prism			Cone
							Torus
							None

Figure 2: The tables (right) present a detailed overview of the train syntax for the trains (top) and blocks (bottom) representation. The accompanying images (left) visually illustrate the individual train attributes of V-LoL and V-LoL.

((2) of Fig. 1 (top)), whereby the class affinity of the sampled train is derived by logical class rule provided by the experimentalist ((4) and (3) of Fig. 1 (top), respectively). Finally, to achieve an equal distribution of east- and westbound trains, V-LoL employs rejection sampling.

Generating images from symbolic trains. A main component for bringing classic, symbolic AI benchmarks into the realm of deep learning is to convert the initially purely symbolic representations into complex visual scenes. Thus, in V-LoL the sampled symbolic trains are rendered into a CLEVR-based [27] environment. Hereby, V-LoL offers two distinct visual representations. On one hand, V-LoL, which comprises images depicting detailed trains that are reminiscent of model trains. On the other hand, V-LoL-Blocks (V-LoL), draws inspiration from the minimalist aesthetics of the CLEVR dataset [27] and presents a simpler visual representation resembling children’s building blocks. Fig. 2 provides an overview of both representations, showcasing the corresponding attributes in the tables and visually illustrating their representation through images. Notably, the number of objects, attributes, and logical versatility remains identical between both, what varies is the complexity of the visual representations. Each train is finally placed in the foreground of an image. V-LoL comes with four default background scenes to choose from that are supported for both the trains and blocks representation: a basic, desert, desert with sky, and fisheye background. Overall, these contain different levels of texture, distortions, and noise. We refer to Fig. 6 in the supplement for their visualizations. Lastly, each image of V-LoL is accompanied with rich ground-truth object information. Each train consists of several cars, which in turn are composed of several train attributes. For each we provide the following information: the position within the scene determined by the centre of the three dimensional object, a binary pixel-wise mask emphasizing the pixels correlated with the train attribute, and its two-dimensional bounding box which surrounds the mask. The depth information of each image are additionally stored. Fig. 6 in the supplement depicts annotations for an example image.

Programmable Logic. Programmable logic is an integral component of V-LoL. By defining various logic rules, one can create a wide range of distinct problems to evaluate AI models regarding their abilities to perform visual logical learning. In fact, we have carefully designed it such that an experimentalist can easily adapt and exchange the underlying logical rule. Leveraging the logical versatility of V-LoL, we have designed a diverse set of challenges to analyze and evaluate the limitations of current AI models. The logic rules employed in these challenges are defined as follows (corresponding prolog and first-order logic (FOL) definitions are available in Sec. B.3 of the supp.): (i) **Theory X:** The train has either a short, closed car or a car with a barrel load is somewhere behind a car with a golden vase load. This rule was originally introduced as ”Theory X” in the new East-West Challenge [4]. (ii) **Numerical rule:** The train has a car where its car position equals its number of payloads which equals its number of wheel axles. (iii) **Complex rule:** Either, there is a car with a car number which is smaller than its number of wheel axles count and smaller than the number of loads, or there is a short and a long car with the same colour where the position number of the short car is smaller than the number of wheel axles of the long car, or the train has three differently

coloured cars. We refer to Tab. 3 in the supp. for more insights on required reasoning properties for each rule.

3 Experiments: AI systems on the V-LoL challenges

Before we dive into the specific evaluation, challenges, and results, we first give an overview on the experimental setup as well as investigated models. We evaluate various AI models from neural, symbolic, and neuro-symbolic AI where we have deliberately chosen methods that encompass a wide range of AI approaches, aiming to gain comprehensive insights into their capabilities and to explore the advantages and disadvantages arising from their different methodologies.

Models. AI approaches that fall under the term **Symbolic AI** (aka Good Old-Fashioned AI (GOFAI) [45]), in general, perform inference on explicit, high-level symbol-based knowledge representations making them well-suited for tasks that require logical reasoning and rule-based decision-making, but ill-suited for inference on low-level data such as raw images. We employ these methods on the symbol-based ground truth information of the V-LoL \rightarrow challenges, assuming the presence of an omniscient perception model. We specifically investigate the abilities of the classical ILP approach, Aleph [52] (*Aleph (Symb)*), and more recent approach, Popper [11] (*Popper (Symb)*). **Neural AI** approaches, on the other hand, perform inference on an implicit, subsymbolic-level knowledge representation and have become the prevailing paradigm in recent years, particularly in visual AI. However, despite their promising predictive performances these approaches have also been shown to be strongly influenced *e.g.* by shortcut behaviour [47] and biases [3], and the degree to which they perform logical reasoning is still an open research topic [55, 9, 46]. In our evaluations we specifically assess the abilities of *ResNet18* [21], *EfficientNet* [54], and Vision Transformer [15] (*ViT*) in handling visual logical learning challenges. **Neuro-Symbolic AI** encompasses a wide range of approaches that follow the idea of combining neural (subsymbolic) with symbolic computations. The motivation behind this is to combine the strengths of both approaches and as such mitigate the shortcomings of the individual methods. The neuro-symbolic models in our evaluations can be categorized into two subcategories (following the categorization of [30]): *Neuro|Symbolic (RCNN-Popper and RCNN-Aleph)* and *Neuro:Symbolic \rightarrow Neuro (α ILP [49])*. Where α ILP utilizes gradients to learn logic rules, *i.e.* differentiable ILP framework, RCNN-Aleph and RCNN-Popper combine their base ILP approach with a Mask-RCNN model [20] that is pretrained on randomly distributed train images for object identification and attribute prediction. In this way, the Mask-RCNN model infers the symbolic representation from an image, that serves as the symbolic input for both ILP approaches. Thus, in comparison to Aleph (Symb.) and Popper (Symb.), RCNN-Aleph and RCNN-Popper can contain possible perception errors stemming from the Mask-RCNN module.

Experimental setup. Unless stated otherwise the training set includes 1k images. All models are trained on specified training splits and evaluated by performing stratified 5-fold cross-validation on a held-out test set, containing 2k images. Quantitative results (unless noted otherwise) correspond to the test set classification accuracy. The hyperparameters for each model are the same over all challenges. Details on these can be found in the supplement (*cf.* Sec. D). Unless specified otherwise, the evaluation datasets were sampled from the Michalski distribution. Finally, runs aborted due to code instabilities, memory overflows, or infinite loops are marked with *.

3.1 V-LoL Challenges

Challenge 1: Visual Perception. In the first challenge, we investigate the robustness of AI models to the visual complexity of V-LoL \rightarrow and V-LoL \square . Here, we create two datasets based on the Theory X class rule on both visual representations, namely the train and the block representation. Fig. 3 presents the final test set accuracies of all AI models on both visualization types. It is evident that the evaluated models exhibit a remarkably similar level of performance on both. In the evaluations conducted on varying scene backgrounds (as shown in Tab. 4 supp.), we also observe only marginal differences in performance. Altogether, these observations suggest that the performance differences between different models in fact stem from the difficulty of the reasoning task, rather than the perceptual difficulty. For the sake of brevity, all further experiments focus exclusively on the more complex train images set in the base scene.

Challenge 2: Logical Reasoning. In the second challenge, we specifically assess the model’s performances in logical reasoning tasks. For this we create datasets of each of the logic rules described

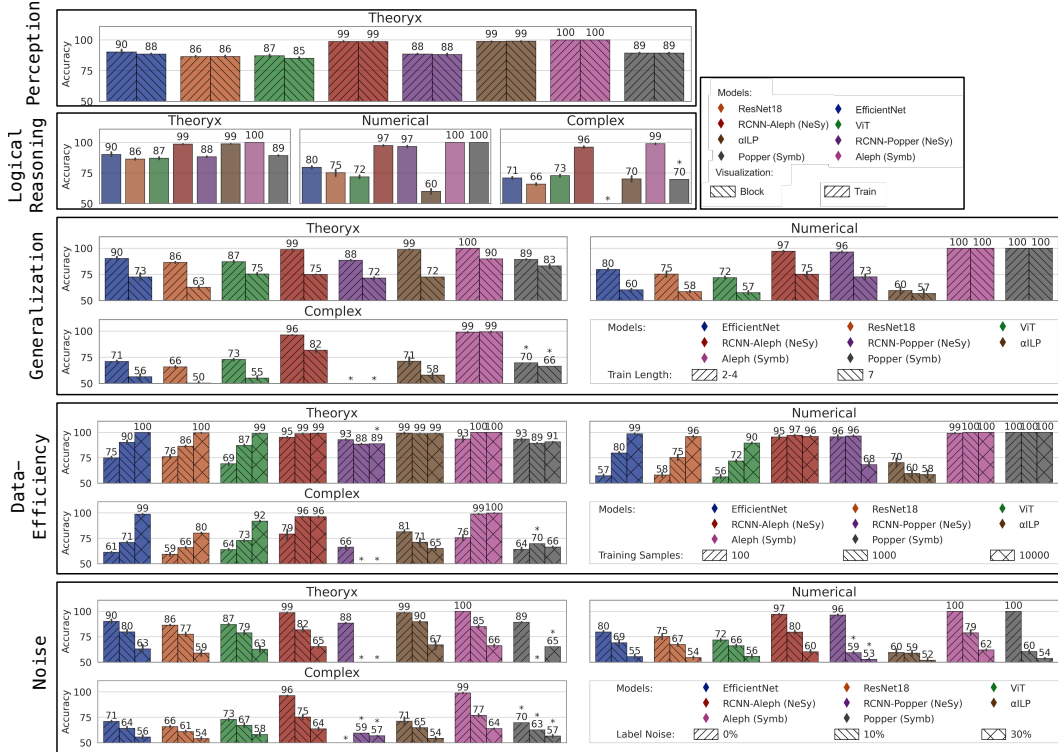


Figure 3: V-LoL challenges. We provide the accuracies of symbolic, neural, and neuro-symbolic AI models achieved in each individual challenge. Each plot depicts the average test accuracy and 95% confidence interval over 5 fold cross-validation. Failed runs are denoted with *.

in Sec. 2.1. Fig. 3 presents the final results on each rule separately. Compared to the previous challenge, it becomes evident that the nature of the logical problems has a more pronounced impact on the performance of the models. Different models exhibit strong variations in their ability to handle the different logical class rules. While the neural approaches demonstrate a decent performance on Theory X, when confronted with the numerical and complex problems they are subject to a severe degradation in performance. This suggests that while these models can identify the attributes of objects, they struggle to understand and reason about numerical information, i.e. making arithmetic comparisons between different concepts, and performing long chains of non-trivial reasoning. Interestingly, α ILP delivered the best performance on Theory X; however, when facing the numeric and complex problems the performance plummeted. In contrast, the Neuro|Symbolic AI systems, RCNN-Popper and RCNN-Aleph, demonstrate much greater abilities in dealing with the numerical problem. Although the purely symbolic AI methods perform even better, they are not truly comparable to the others, as they lack the ability to handle the visual component of V-LoL in the first place. In this regard, the Neuro|Symbolic AI methods show a relatively robust behaviour with minor losses in performance over the different logical rules. However, RCNN-Popper failed to learn the complex problem due to endless loops and code instabilities during execution. Since Popper was able to fit on the symbolic ground truth of the dataset, this issue is probably caused by to combination of the rule complexity and perception noise caused by the RCNN module. In general, all models face the greatest challenge when dealing with the complex rule, emphasising the complexity of the rule, which is reflected in the level of reasoning required to solve the task.

Challenge 3: Generalization. One would assume that models that truly solved the logical learning problems should be able to demonstrate this ability even on train compositions not seen during training. To evaluate this, in challenge 3 we evaluate models that were trained on images with trains encompassing up to four cars on a test set of trains consisting of 7 cars. The results in Fig. 3, reveal the limitations of the evaluated models in terms of generalization. Despite showing promising performances in the previous challenges, almost all models struggle to generalize effectively to longer train scenarios. This suggests a limited ability to adapt their reasoning capabilities to challeng-

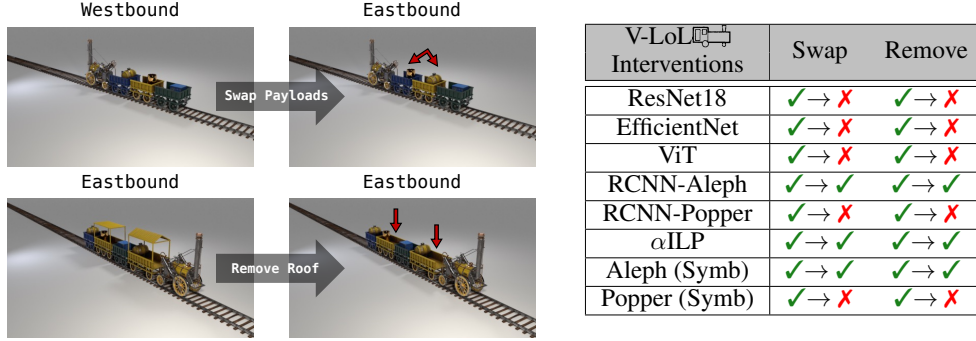
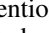


Figure 4: Interventions (challenge 4). We analyze the impact of test-time interventions on the models’ classification. The first evaluated intervention involves swapping the payloads (top). The second involves removing the roofs (bottom). The table provides insights into each models’ classification, before and after intervention, where a green check indicates correct and a red cross incorrect class prediction.

ing, unseen inputs. Instead of comprehending the underlying problem and performing appropriate reasoning, the models tend to approximate the data distribution of the training set, leading to sub-optimal generalization. We further evaluated the neural models on an additional dataset, where the trains were sampled from the random attribute distribution rather than the Michalski distribution used in the training set. The results of Fig. 7 in the supp. indicate that the neural models learn strong correlations between the attributes, but lack the ability to generalize to out-of-distribution inputs. Specifically over all three models, when evaluated on images that stem from the uniformly distributed attribute distribution we observed a performance drop to close to random guessing.

Challenge 4: Test-Time Interventions. In challenge 4, we leverage the versatility provided by V-LoL  that allows for performing test-time interventions on the composition of individual trains. In this way we investigate the model’s learned knowledge by conducting two interventions on images of the Theory X challenge. Specifically, we investigate the class predictions for two example images of the test set on which we perform two different attribute interventions. In the first intervention (*cf.* Fig. 4 (top left)), we swap the position of two payloads, resulting in the barrel being placed behind the golden vase and thus changing the underlying class from west- to eastbound. For the second intervention, we remove class-irrelevant artefacts in the form of the roofs of the first and third car (*cf.* Fig. 4 (bottom left)). The table in Fig. 4 (right) presents the prediction performance of all models on these two exemplary images (check indicates a correct, a cross incorrect prediction). While all models are able to correctly classify the original (pre-intervention) images, many struggle to handle the intervened images. Especially the neural models are easily fooled by the interventions. This suggests that they do not fully capture the underlying logical learning problem. Interestingly, the neuro-symbolic models RCNN-Aleph and α ILP, appear less affected by these interventions.

Challenge 5: Data-Efficiency. Challenge 5 investigates the data efficiency of the individual models by assessing their performances across different training set sizes. The evaluation is conducted using varying numbers of training samples, namely 100, 1k, and 10k. As depicted in Fig. 3 in the small data regime, we observe notable variations in performances among the models. While the neural models are subject to severe performance degradation, the neuro-symbolic approaches showcase their ability to learn effectively also from small amounts of data. In particular, it can be observed that α ILP achieves best performances on both Theory X and complex problems for 100 training samples. Intriguingly, these performances even surpass those achieved with 1k samples. Turning our attention to the large data regime (10k training samples), we note substantial performance improvements for neural approaches. On the other hand, the neuro-symbolic AI systems encounter challenges in effectively scaling their performances as α ILP and Popper exhibit declines in performance. Popper additionally runs into endless loops and code instabilities during execution. Noteworthy, Aleph, on the other hand, suffers from poor optimization, leading to excessive memory usage (up to 1 TB RAM) and prolonged training iterations. Notably, α ILP consistently performs poorly on the numerical problem. This could potentially be attributed to issues with mode declaration and hyperparameter tuning. Comparing the individual rules across the training size, it becomes evident that the complex rule generally poses the greatest challenge.

Challenge 6: Label Noise. In the final challenge, we investigate the robustness of the AI models to label noise. For this purpose, the respective AI systems are trained on datasets with specific amounts of perturbed labels (flipped labels). In Fig. 3, we compare the model’s performances for different degrees of label perturbation. In general, all AI models have difficulties coping with the noise. In this experiment α ILP seems to be least affected given the Theory X rule. On numerical and complex problems the ILP system Aleph maintains its lead position, although it also has to cope with large performance losses. The other ILP system Popper, however, is subject to strong turmoil that results in a performance close to random guessing. The investigated neural approaches all show a very similar level of degradation and are slightly less affected by the noise compared to ILP.

Discussion. In our analysis we have evaluated and compared a range of AI architectures, and revealed several key shortcomings. While the **symbolic AI** models demonstrate strong performances across different visual logical learning problems (*e.g.* challenge 2), it must be noted that they assume omniscient perception and are subject to certain challenges requiring excessive tuning of hyperparameters and priors (language biases), where even minor changes can lead to significant performance fluctuations. In addition, the application faces limitations that are particularly pronounced when dealing with noise or larger training samples (challenge 5 and 6) such as code instabilities, endless loops or excessive memory usage. The **neural AI** models show largely similar performances amongst themselves across the different challenges. While they can identify the attributes of objects, they struggle to reason about numerical information, *e.g.* making arithmetic comparisons between different concepts, as well as performing long chains of intricate reasoning (*cf.* challenge 2). These models tend to acquire pronounced biases from the training data, leading to challenges in overcoming these biases when confronted with data outside the training distribution. Challenge 4 particularly reveals that these models tend to be susceptible to small changes in input, being easily fooled by significant or insignificant perturbations in train compositions. Additionally, training on different dataset sizes exposes their reliance on a large training set size (challenge 5). The investigated **neuro-symbolic AI** models exhibit rather similar performances and limitations amongst themselves, but are also comparable to the performances of the symbolic AI models, albeit are influenced by the noise added through their perception modules. Despite specific limitations (*e.g.* α ILP’s difficulties with the numerical and complex problem), their abilities to flexibly handle the visual component *and* logical reasoning components of the challenges makes them attractive approaches that lie between the purely neural and symbolic models.

4 Impact

The V-LoL dataset is related to datasets on visual reasoning from the field of deep learning, but also to classic symbolic AI benchmarks. Importantly, it has an impact on various subfields of AI.

Visual (reasoning) datasets. The transition from purely visual perception tasks to visual reasoning has led to the development of specialized datasets that challenge AI models to perform different reasoning tasks based on visual information. Notable examples include VQA [1, 56, 31, 27], QAR [25], CLEVRER [58], CLEVR-Hans [53], MNIST-Addition [35], GQA dataset [26], PTR dataset [24], and RAVEN dataset [7]. A comparison of a selection of datasets, their features and learning tasks can be found in Tab. 1. While most of these tasks assume pre-defined programs to compute answers, V-LoL takes a different approach by requiring agents to learn abstract programs for classification, adding a unique dimension to the field of visual reasoning.

Classical ILP benchmarks. ILP benchmarks have a long-standing history and have been an integral part of the AI field since its inception, serving as standardized tasks to evaluate AI systems’ performance in logical learning and knowledge representation. These benchmarks involve learning logical rules or programs from examples and background knowledge, encompassing challenges such as logical inference, relational reasoning, and generalization from limited examples. Examples of popular ILP benchmarks include the Michalski train problem [37, 38], Bongard Problems [5], Kinship [16], Mutagenesis [14], and Bongard-LOGO [42].

AI systems. V-LoL has the distinct advantage of allowing the evaluation and comparison of AI systems from the domains of symbolic, neural, and neuro-symbolic AI. Symbolic AI, utilizing representations like First-Order Logic (FOL), provides essential knowledge representation and reasoning capabilities [2, 6, 41]. ILP has been established as a technique to learn generalized rules using FOL as its language [40, 43, 13, 10], offering advantages such as learning explicit programs and

learning from small data. Deep Learning, a prominent technique in neural AI, has shown significant achievements in various AI tasks [32, 50, 28], although lacking interpretable and explainable reasoning steps. The emerging field of neuro-symbolic AI integrates symbolic computations and neural networks [18], enabling efficient parameter estimation (e.g. DeepProbLog [35], NeurASP [57], SLASH [51], NS-CL [36], and differentiable theorem provers [44]) and explicit logic program learning from raw data (e.g. ∂ ILP [17], α ILP [49], and FFNSL [12]). V-LoL serves as a diagnostic benchmark for evaluating and advancing AI systems across all of these different domains.

5 Conclusion

We have introduced V-LoL, a dataset specifically designed for the diagnostic evaluation of visual logical learning in AI models. Specifically, V-LoL $\mathbb{L}\rightarrow\mathbb{L}$, an initial instantiation of V-LoL, provides a versatile generator that allows to generate custom datasets for detailed investigations of the capabilities and limitations of current and future AI models. In this way it is possible to investigate various learning abilities of AI models, ranging from perception and relational reasoning to arithmetic reasoning and test-set generalization. In this context, V-LoL $\mathbb{L}\rightarrow\mathbb{L}$ offers the ability to finely adjust the learning task, enabling a comprehensive analysis going beyond existing benchmarks. We have evaluated several symbolic, neural, and neuro-symbolic models and could identify several key shortcomings and benefits arising from the individual methodologies. By merging logic and vision, V-LoL specifically poses an attractive tool for ongoing research efforts aimed at enhancing the performance and capabilities of AI models, and further driving progress in visual logical learning.

Future evaluations include assessing the visual logical learning capabilities of large-scale vision-language. Investigating the models' generalization across different background scenes can provide crucial information on their robustness to out-of-distribution data. Furthermore, conducting extensive human evaluations will provide unique perspectives on the challenges posed by V-LoL. Finally, extending V-LoL to include other ILP problems, but also moving to the domain of 3D image sequences are important directions for future research.

References

- [1] Stanislaw Antol, Aishwarya Agrawal, Jiasen Lu, Margaret Mitchell, Dhruv Batra, C. Lawrence Zitnick, and Devi Parikh. VQA: visual question answering. In *International Conference on Computer Vision (ICCV)*, pages 2425–2433. IEEE Computer Society, 2015. 1, 3, 8
- [2] Chitta Baral. *Knowledge Representation, Reasoning and Declarative Problem Solving*. Cambridge University Press, 2010. 8
- [3] Emily M. Bender, Timnit Gebru, Angelina McMillan-Major, and Shmargaret Shmitchell. On the dangers of stochastic parrots: Can language models be too big? In *Conference on Fairness, Accountability, and Transparency (FAccT)*, pages 610–623. ACM, 2021. 5
- [4] Eric Bloedorn, Ibrahim F Imam, Kenneth A Kaufman, Marcus A Maloof, Ryszard S Michalski, and Janusz Wnek. How did aq face the east-west challenge? an analysis of the aq family's performance in the 2nd international competition of machine learning programs. Technical report, 1995. 4, 13
- [5] Mikhail Moiseevich Bongard. The recognition problem. Technical report, Foreign Technology Div Wright-Patterson AFB Ohio, 1968. 8
- [6] Ronald Brachman and Hector Levesque. *Knowledge representation and reasoning*. Elsevier, 2004. 8
- [7] Patricia Carpenter, Marcel Just, and Peter Shell. What one intelligence test measures: A theoretical account of the processing in the raven progressive matrices test. *Psychological Review*, 97:404–31, 08 1990. 8
- [8] Marius Cordts, Mohamed Omran, Sebastian Ramos, Timo Rehfeld, Markus Enzweiler, Rodrigo Benenson, Uwe Franke, Stefan Roth, and Bernt Schiele. The cityscapes dataset for semantic urban scene understanding. In *Conference on Computer Vision and Pattern Recognition (CVPR)*, pages 3213–3223. IEEE Computer Society, 2016. 1
- [9] Antonia Creswell, Murray Shanahan, and Irina Higgins. Selection-inference: Exploiting large language models for interpretable logical reasoning. *CoRR*, abs/2205.09712, 2022. 5
- [10] Andrew Cropper, Sebastijan Dumancic, and Stephen H. Muggleton. Turning 30: New ideas in inductive logic programming. In *International Joint Conference on Artificial Intelligence (IJCAI)*, pages 4833–4839, 2020. 8
- [11] Andrew Cropper and Rolf Morel. Learning programs by learning from failures, 2020. 5
- [12] Daniel Cunningham, Mark Law, Jorge Lobo, and Alessandra Russo. FFNSL: feed-forward neural-symbolic learner. *Machine Learning*, 112(2):515–569, 2023. 9
- [13] Luc De Raedt and Kristian Kersting. *Probabilistic Inductive Logic Programming*, pages 1–27. Springer Berlin Heidelberg, 2008. 8

- [14] A. K. Debnath, R. L. Lopez de Compadre, G. Debnath, A. J. Shusterman, and C. Hansch. Structure-activity relationship of mutagenic aromatic and heteroaromatic nitro compounds. Correlation with molecular orbital energies and hydrophobicity. *Journal of medicinal chemistry*, 34(2):786–797, 1991. 8
- [15] Alexey Dosovitskiy, Lucas Beyer, Alexander Kolesnikov, Dirk Weissenborn, Xiaohua Zhai, Thomas Unterthiner, Mostafa Dehghani, Matthias Minderer, Georg Heigold, Sylvain Gelly, Jakob Uszkoreit, and Neil Houlsby. An image is worth 16x16 words: Transformers for image recognition at scale. In *International Conference on Learning Representations (ICLR)*, 2021. 5
- [16] Dheeru Dua and Casey Graff. UCI machine learning repository, 2017. 1, 8
- [17] Richard Evans and Edward Grefenstette. Learning explanatory rules from noisy data. *Journal of Artificial Intelligence Research*, 61:1–64, 2018. 9
- [18] Artur Garcez and Luís Lamb. Neurosymbolic ai: the 3rd wave. *Artificial Intelligence Review*, pages 1–20, 03 2023. 9
- [19] Timnit Gebru, Jamie Morgenstern, Briana Vecchione, Jennifer Wortman Vaughan, Hanna M. Wallach, Hal Daumé III, and Kate Crawford. Datasheets for datasets. *Communications of the ACM*, 64(12):86–92, 2021. 19
- [20] Kaiming He, Georgia Gkioxari, Piotr Dollár, and Ross B. Girshick. Mask R-CNN. In *International Conference on Computer Vision (ICCV)*, pages 2980–2988. IEEE Computer Society, 2017. 5
- [21] Kaiming He, Xiangyu Zhang, Shaoqing Ren, and Jian Sun. Deep residual learning for image recognition. In *Conference on Computer Vision and Pattern Recognition (CVPR)*, pages 770–778. IEEE Computer Society, 2016. 5
- [22] Andreas Holzinger, Michael D. Kickmeier-Rust, and Heimo Müller. KANDINSKY patterns as iq-test for machine learning. In Andreas Holzinger, Peter Kieseberg, A Min Tjoa, and Edgar R. Weippl, editors, *International Cross-Domain Conference Machine Learning and Knowledge Extraction (CD-MAKE)*, volume 11713, pages 1–14. Springer, 2019. 3
- [23] Andreas Holzinger, Anna Saranti, and Heimo Mueller. Kandinskypatterns—an experimental exploration environment for pattern analysis and machine intelligence. *CoRR*, 2021. 3
- [24] Yining Hong, Li Yi, Josh Tenenbaum, Antonio Torralba, and Chuang Gan. PTR: A benchmark for part-based conceptual, relational, and physical reasoning. In *Conference on Neural Information Processing Systems (NeurIPS)*, pages 17427–17440, 2021. 1, 3, 8
- [25] Jiani Huang, Ziyang Li, Binghong Chen, Karan Samel, Mayur Naik, Le Song, and Xujie Si. Scallop: From probabilistic deductive databases to scalable differentiable reasoning. In *Conference on Neural Information Processing (NeurIPS)*, pages 25134–25145, 2021. 8
- [26] Drew A. Hudson and Christopher D. Manning. GQA: A new dataset for real-world visual reasoning and compositional question answering. In *Conference on Computer Vision and Pattern Recognition (CVPR)*, pages 6700–6709. Computer Vision Foundation / IEEE, 2019. 1, 8
- [27] Justin Johnson, Bharath Hariharan, Laurens van der Maaten, Li Fei-Fei, C. Lawrence Zitnick, and Ross B. Girshick. CLEVR: A diagnostic dataset for compositional language and elementary visual reasoning. In *Conference on Computer Vision and Pattern Recognition (CVPR)*, pages 1988–1997. IEEE Computer Society, 2017. 1, 2, 3, 4, 8
- [28] John Jumper, Richard Evans, Alexander Pritzel, Tim Green, Michael Figurnov, Olaf Ronneberger, Kathryn Tunyasuvunakool, Russ Bates, Augustin Židek, Anna Potapenko, Alex Bridgland, Clemens Meyer, Simon A A Kohl, Andrew J Ballard, Andrew Cowie, Bernardino Romera-Paredes, Stanislav Nikolov, Rishub Jain, Jonas Adler, Trevor Back, Stig Petersen, David Reiman, Ellen Clancy, Michal Zielinski, Martin Steinegger, Michalina Pacholska, Tamas Berghammer, Sebastian Bodenstern, David Silver, Oriol Vinyals, Andrew W Senior, Koray Kavukcuoglu, Pushmeet Kohli, and Demis Hassabis. Highly accurate protein structure prediction with AlphaFold. *Nature*, 596(7873):583–589, 2021. 9
- [29] Laurynas Karazija, Iro Laina, and Christian Rupprecht. Clevrtex: A texture-rich benchmark for unsupervised multi-object segmentation. In *Conference on Neural Information Processing Systems (NeurIPS), NeurIPS Datasets and Benchmarks*, 2021. 1
- [30] Henry Kautz. The third ai summer: Aaai robert s. engelmore memorial lecture. *AI Magazine*, 43(1):105–125, Mar. 2022. 5
- [31] Ranjay Krishna, Yuke Zhu, Oliver Groth, Justin Johnson, Kenji Hata, Joshua Kravitz, Stephanie Chen, Yannis Kalantidis, Li-Jia Li, David A. Shamma, Michael S. Bernstein, and Li Fei-Fei. Visual genome: Connecting language and vision using crowdsourced dense image annotations. *International Journal of Computer Vision*, 123(1):32–73, 2017. 8
- [32] Yann LeCun, Yoshua Bengio, and Geoffrey Hinton. Deep learning. *Nature*, 521(7553):436, 2015. 9
- [33] Yanghao Li, Saining Xie, Xinlei Chen, Piotr Dollár, Kaiming He, and Ross B. Girshick. Benchmarking detection transfer learning with vision transformers. *CoRR*, abs/2111.11429, 2021. 18
- [34] Tsung-Yi Lin, Michael Maire, Serge J. Belongie, James Hays, Pietro Perona, Deva Ramanan, Piotr Dollár, and C. Lawrence Zitnick. Microsoft COCO: common objects in context. In *European Conference on Computer Vision (ECCV)*, volume 8693, pages 740–755. Springer, 2014. 1
- [35] Robin Manhaeve, Sebastijan Dumancic, Angelika Kimmig, Thomas Demeester, and Luc De Raedt. Deep-problog: Neural probabilistic logic programming. In *Conference on Neural Information Processing Systems (NeurIPS)*, pages 3753–3763, 2018. 8, 9
- [36] Jiayuan Mao, Chuang Gan, Pushmeet Kohli, Joshua B. Tenenbaum, and Jiajun Wu. The neuro-symbolic concept learner: Interpreting scenes, words, and sentences from natural supervision. In *International Conference on Learning Representations (ICLR)*, 2019. 9

- [37] Ryszard S. Michalski. Pattern recognition as rule-guided inductive inference. *IEEE Transactions on Pattern Analysis and Machine Intelligence*, PAMI-2(4):349–361, 1980. 1, 2, 3, 8, 13
- [38] Donald Michie, Stephen Muggleton, David L. Page, and Ashwin Srinivasan. To the international computing community: A new east-west challenge. 1994. 1, 8
- [39] Stephen Muggleton. Random train generator, 1998. 3, 14
- [40] Stephen H. Muggleton. Inverse entailment and prolog. *New Generation Computing*, 13(3&4):245–286, 1995. 3, 8
- [41] Maximilian Nickel, Kevin Murphy, Volker Tresp, and Evgeniy Gabrilovich. A review of relational machine learning for knowledge graphs. *Proceedings of the IEEE*, 104(1):11–33, 2015. 8
- [42] Weili Nie, Zhiding Yu, Lei Mao, Ankit B. Patel, Yuke Zhu, and Anima Anandkumar. Bongard-logo: A new benchmark for human-level concept learning and reasoning. In *Conference on Neural Information Processing Systems (NeurIPS)*, 2020. 8
- [43] Shan-Hwei Nienhuys-Cheng, Ronald de Wolf, J. Siekmann, and J. G. Carbonell. *Foundations of Inductive Logic Programming*. Springer-Verlag, 1997. 8
- [44] Tim Rocktäschel and Sebastian Riedel. End-to-end Differentiable Proving. In *Conference on Neural Information Processing (NeurIPS)*, pages 3788–3800, 2017. 9
- [45] Stuart Russell and Peter Norvig. *Artificial Intelligence: A Modern Approach (4th Edition)*. Pearson, 2020. 5
- [46] Abulhair Saparov and He He. Language models are greedy reasoners: A systematic formal analysis of chain-of-thought. *CoRR*, abs/2210.01240, 2022. 5
- [47] Patrick Schramowski, Wolfgang Stammer, Stefano Teso, Anna Brugger, Franziska Herbert, Xiaoting Shao, Hans-Georg Luigs, Anne-Katrin Mahlein, and Kristian Kersting. Making deep neural networks right for the right scientific reasons by interacting with their explanations. *Nature Machine Intelligence*, 2(8):476–486, 2020. 5
- [48] Christoph Schuhmann, Romain Beaumont, Richard Vencu, Cade Gordon, Ross Wightman, Mehdi Cherti, Theo Coombes, Aarush Katta, Clayton Mullis, Mitchell Wortsman, Patrick Schramowski, Srivatsa Kundurthy, Katherine Crowson, Ludwig Schmidt, Robert Kaczmarczyk, and Jenia Jitsev. LAION-5B: an open large-scale dataset for training next generation image-text models. In *Conference on Neural Information Processing Systems (NeurIPS)*, 2022. 1
- [49] Hikaru Shindo, Viktor Pfanschilling, Devendra Singh Dhami, and Kristian Kersting. α lp: thinking visual scenes as differentiable logic programs. *Machine Learning*, 112(5):1465–1497, May 2023. 5, 9
- [50] David Silver, Aja Huang, Christopher J. Maddison, Arthur Guez, Laurent Sifre, George van den Driessche, Julian Schrittwieser, Ioannis Antonoglou, Veda Panneershelvam, Marc Lanctot, Sander Dieleman, Dominik Grewe, John Nham, Nal Kalchbrenner, Ilya Sutskever, Timothy Lillicrap, Madeleine Leach, Koray Kavukcuoglu, Thore Graepel, and Demis Hassabis. Mastering the game of go with deep neural networks and tree search. *Nature*, 529:484–503, 2016. 9
- [51] Arseny Skryagin, Wolfgang Stammer, Daniel Ochs, Devendra Singh Dhami, and Kristian Kersting. Neural-probabilistic answer set programming. In Gabriele Kern-Isberner, Gerhard Lakemeyer, and Thomas Meyer, editors, *International Conference on Principles of Knowledge Representation and Reasoning (KR)*, 2022. 9
- [52] A. Srinivasan. *The Aleph Manual*, 2001. 5
- [53] Wolfgang Stammer, Patrick Schramowski, and Kristian Kersting. Right for the right concept: Revising neuro-symbolic concepts by interacting with their explanations. In *Conference on Computer Vision and Pattern Recognition (CVPR)*, pages 3619–3629. Computer Vision Foundation / IEEE, 2021. 3, 8
- [54] Mingxing Tan and Quoc V. Le. Efficientnetv2: Smaller models and faster training. In *International Conference on Machine Learning (ICML)*, volume 139 of *Proceedings of Machine Learning Research*, pages 10096–10106. PMLR, 2021. 5
- [55] Jason Wei, Xuezhi Wang, Dale Schuurmans, Maarten Bosma, Brian Ichter, Fei Xia, Ed H. Chi, Quoc V. Le, and Denny Zhou. Chain-of-thought prompting elicits reasoning in large language models. In *Conference on Neural Information Processing (NeurIPS)*, 2022. 5
- [56] Qi Wu, Damien Teney, Peng Wang, Chunhua Shen, Anthony Dick, and Anton Van Den Hengel. Visual question answering: A survey of methods and datasets. *Computer Vision and Image Understanding*, 163:21–40, 2017. 8
- [57] Zhun Yang, Adam Ishay, and Joohyung Lee. Neurasp: Embracing neural networks into answer set programming. In *International Joint Conference on Artificial Intelligence (IJCAI)*, pages 1755–1762, 2020. 9
- [58] Kexin Yi, Chuang Gan, Yunzhu Li, Pushmeet Kohli, Jiajun Wu, Antonio Torralba, and Joshua B. Tenenbaum. Clevrer: Collision events for video representation and reasoning. In *International Conference on Learning Representations (ICLR)*, 2020. 8
- [59] Rowan Zellers, Yonatan Bisk, Ali Farhadi, and Yejin Choi. From recognition to cognition: Visual commonsense reasoning. In *Conference on Computer Vision and Pattern Recognition (CVPR)*, pages 6720–6731. Computer Vision Foundation / IEEE, 2019. 1
- [60] Chi Zhang, Feng Gao, Baoxiong Jia, Yixin Zhu, and Song-Chun Zhu. RAVEN: A dataset for relational and analogical visual reasoning. In *Conference on Computer Vision and Pattern Recognition (CVPR)*, pages 5317–5327. Computer Vision Foundation / IEEE, 2019. 1, 3
- [61] Yuke Zhu, Oliver Groth, Michael S. Bernstein, and Li Fei-Fei. Visual7w: Grounded question answering in images. In *Conference on Computer Vision and Pattern Recognition (CVPR)*, pages 4995–5004. IEEE

Checklist

1. For all authors...
 - (a) Do the main claims made in the abstract and introduction accurately reflect the paper's contributions and scope? [Yes]
 - (b) Did you describe the limitations of your work? [Yes] See supplements.
 - (c) Did you discuss any potential negative societal impacts of your work? [Yes] See supplements.
 - (d) Have you read the ethics review guidelines and ensured that your paper conforms to them? [Yes]
2. If you are including theoretical results...
 - (a) Did you state the full set of assumptions of all theoretical results? [N/A]
 - (b) Did you include complete proofs of all theoretical results? [N/A]
3. If you ran experiments (e.g. for benchmarks)...
 - (a) Did you include the code, data, and instructions needed to reproduce the main experimental results (either in the supplemental material or as a URL)? [Yes] See supplements and linked github URLs.
 - (b) Did you specify all the training details (e.g., data splits, hyperparameters, how they were chosen)? [Yes]
 - (c) Did you report error bars (e.g., with respect to the random seed after running experiments multiple times)? [Yes]
 - (d) Did you include the total amount of compute and the type of resources used (e.g., type of GPUs, internal cluster, or cloud provider)? [Yes]
4. If you are using existing assets (e.g., code, data, models) or curating/releasing new assets...
 - (a) If your work uses existing assets, did you cite the creators? [Yes] See the supplements.
 - (b) Did you mention the license of the assets? [Yes]
 - (c) Did you include any new assets either in the supplemental material or as a URL? [No]
 - (d) Did you discuss whether and how consent was obtained from people whose data you're using/curating? [N/A]
 - (e) Did you discuss whether the data you are using/curating contains personally identifiable information or offensive content? [N/A]
5. If you used crowdsourcing or conducted research with human subjects...
 - (a) Did you include the full text of instructions given to participants and screenshots, if applicable? [N/A]
 - (b) Did you describe any potential participant risks, with links to Institutional Review Board (IRB) approvals, if applicable? [N/A]
 - (c) Did you include the estimated hourly wage paid to participants and the total amount spent on participant compensation? [N/A]

Supplemental Materials

A Ethical Statement and Limitations

Ethical Statement. The V-LoL dataset is a diagnostic dataset aimed at explicitly investigating various challenges of visual logical learning and in this way is designed to identify the capabilities and potential shortcomings of AI models. It should thus also serve as a benchmark for improving AI models in general. Although it is therefore not its intention, providing such a benchmark can also have the effect *e.g.* of improving models that are to be used in a harmful way. However, our work or implications thereof do not, to the best of our knowledge, pose an obvious direct threat to any individuals or society in general. In addition, as the introduced datasets are synthetically generated no harm was done in the generation of the dataset.

Limitations. A main limitation of our work is the synthetic character of our dataset, in comparison to the visual complexity of natural images. This synthetic character, however, allows for great versatility and generation power, *e.g.* the direct access to the data generation process allows for easily performing test-time interventions, an important property for targeted evaluations of the visual logical learning abilities of AI models. A further limitation is missing evaluations on more recent (pre-trained) large language or multi-modal models. However, we consider a thorough analysis of these models on our benchmark as future work.

B V-LoL dataset

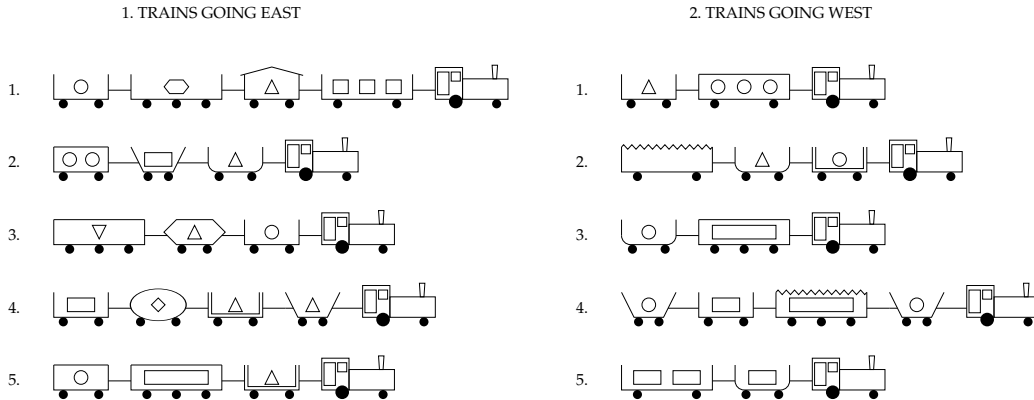


Figure 5: Michalski's original set of trains [37]

B.1 Details on Michalski Train Semantics

E. Bloedorn et al.[4] state, that Muggleton's Prolog representation shows subtle differences to the original representation from Michalski such that artefacts are created which are not present in Michalski's original work. These artefacts result from an ambiguous definition of the individual descriptors. Consequently, depicted cars without a load must be assigned a description of the load shape, even though the number of loads remains zero. In this sense, any load shape can be assigned to a car without visually affecting the depicted car. This is an inconsistency that is not present in the original Michalski trains. However, as the images contain unambiguous information about the train, it is not present in the visual V-LoL classification task. Nevertheless, it is beneficial to remove this inconsistency in the background knowledge of the dataset. In V-LoL we circumvent this problem by introducing the value "none" for the load shape descriptor.

Table 2: Attributes of Michalski’s original train attributes. The Table gives an overview of the original assignable values of each descriptor. For the respective descriptors, the above-mentioned interrelationships must be taken into account such that some attributes might be mutually exclusive.

Car Position	Car Shape	Car Length	Car Wall	Car Roof	Wheels Num.	Load Num.	Load Shape
1	Rectangle	Short	Single	None	2	0	Rectangle
2	Bucket	Long	Double	Arc	3	1	Triangle
3	Ellipse			Flat		2	Circle
4	Hexagon			Jagged		3	Diamond
	U shaped			Peaked			Hexagon
							U-triangle

Trains sampled from the random distribution can be generated in one of 23.4 trillion combinations, assuming a train length of 2 - 4 cars. This number of permutations grows exponentially with every additional car.

B.2 Attribute Constraints

In the following we list the attribute constraints that are enforced via Muggleton’s [39] Prolog train generator:

1. A train has two, three or four cars, each of which can either be long or short.
2. A long car can have either two or three axles.
3. A short car can be rectangular, u-shaped, bucket-shaped, hexagonal, or elliptical, while a long car must be rectangular.
4. A hexagonal or elliptical car is necessarily closed, while any other car can be either open or closed.
5. The roof of a long-closed car can be either flat or jagged.
6. The roof of a hexagonal car is necessarily flat, while the roof of an elliptical car is necessarily an arc. Any other short closed car can have either a flat or a peaked roof.
7. If a short car is rectangular then it can also be double-sided.
8. A long car can be empty or it can contain one, two or three replicas of one of the following kinds of load: circle, inverted-triangle, hexagon, or rectangle.
9. A short car contains either one or two replicas of the following kinds of load: circle, triangle, rectangle, or diamond.
10. No sub-distinctions are drawn among rectangular loads, even though some are drawn square and others more or less oblong. The presumption is that they are drawn just as oblong as they need to be in each case to fill the available container space.
11. In Michalski’s original version a possible distinction between hollow and solid wheels was ignored, as also here.

B.3 Prolog and FOL Notation of the Classification rules

In the following we provide the Prolog and first-order-logic (FOL) representations of the Theory X, Numerical and Complex logic rules that were used in our evaluations.

Theory X is defined as follows:

$$\begin{aligned}
 eastbound(Train) \models & \exists Car_1, Car_2, \\
 & has-car(Train, Car_1) \wedge has-car(Train, Car_2) \\
 & \wedge ((short(Car_1) \wedge closed(Car_1)) \\
 & \vee (has-load(Car_1, golden-vase)
 \end{aligned}$$

$$\begin{aligned} &\wedge \text{has-load}(\text{Car}_2, \text{barrel}) \\ &\wedge \text{somewhere-behind}(\text{Train}, \text{Car}_2, \text{Car}_1)) \end{aligned}$$

Prolog:

```
eastbound([Car|Cars]):- (short(Car), closed(Car));
(has_load0(Car,triangle),has_load1(Cars,circle));
eastbound(Cars).
```

The numerical rule is defined as follows:

$$\begin{aligned} \text{eastbound}(\text{Train}) \models \exists \text{Car}_1 \text{ has-car}(\text{Train}, \text{Car}_1) \wedge \text{load-num}(\text{Car}_1, N) \\ \wedge \text{car-num}(\text{Car}_1, N) \wedge \text{has-wheel}(\text{Car}_1, N) \end{aligned}$$

Prolog:

```
eastbound(Train):- has_car(Train,Car),load_num(Car,N), car_num(Car,N),
has_wheel0(Car,N).
```

The complex rule is defined as follows:

$$\begin{aligned} \text{eastbound}(\text{Train}) \models \exists \text{Car}_1, \text{Car}_2, \text{Car}_3 \\ \text{has-car}(\text{Train}, \text{Car}_1) \wedge (\text{has-car}(\text{Train}, \text{Car}_2) \wedge \text{has-car}(\text{Train}, \text{Car}_3) \wedge \\ (\text{load-num}(\text{Car}_1, N1) \wedge \text{car-num}(\text{Car}_1, N2) \wedge \\ \text{has-wheel0}(\text{Car}_1, N3) \wedge (N2 < N1) \wedge (N2 < N3)) \\ \vee (\text{short}(\text{Car}_1) \wedge \text{long}(\text{Car}_2) \wedge \text{car-num}(\text{Car}_1, N1) \wedge \text{car-color}(\text{Car}_1, A) \wedge \\ \text{car-color}(\text{Car}_2, A) \wedge \text{has-wheel}(\text{Car}_2, N2) \wedge (N1 < N2)) \\ \vee (\text{car-color}(\text{Car}_1, X) \wedge \text{car-color}(\text{Car}_2, Y) \wedge \text{car-color}(\text{Car}_3, Z) \wedge \\ \neg(X = Y) \wedge \neg(Y = Z) \wedge \neg(Z = X)) \end{aligned}$$

Prolog:

```
eastbound(Train):-
has_car(Train,Car1),has_car(Train,Car2), has_car(Train,Car3),
(load_num(Car1,N1), car_num(Car1,N2),has_wheel0(Car1,N3), N2 < N1, N2 < N3;
short(Car1), long(Car2),car_num(Car1,N1), car_color(Car1, A),
car_color(Car2, A),has_wheel0(Car2,N2), N1 < N2;
car_color(Car1,X), car_color(Car2,Y),car_color(Car3,Z),X/=Y, Y/=Z, Z/=X).
```

B.4 Reasoning Properties for Logic Rules

Successfully solving the individual V-LoL challenges requires a set of learning and reasoning abilities, including:

- **Object recognition** is a crucial component of visual reasoning and involves identifying and categorizing objects based on their physical attributes.
- **Counting** is also an essential skill in the domain of visual reasoning, which involves determining and understanding the number of objects or occurrences of a particular feature. In the case of V-LoL it is required to accurately count the number of occurrences of objects and concepts such as the number of cars, payloads or car axles.
- **Relational reasoning** is another essential type of reasoning which involves understanding and drawing conclusions based on relationships between multiple objects and concepts. For example, understanding that a barrel load is always located in a car in front of a car with a golden vase load.
- **Spatial reasoning** involves drawing conclusions based on the spatial information of individual objects within a scene. E.g. in V-LoL it is required to understand and conclude which car is in front of another in the direction of travel, i.e. in the direction of the locomotive.

Table 3: The V-LoL-Trains problems and the visual logical learning challenges that they address individually. We here categorize based on *object recognition* and *counting* abilities and *relational*, *spatial*, *analogical*, *arithmetic*, *abstract* and *exact* logical reasoning. For each of our three V-LoL-Trains classification challenges, “Theory X”, “Numerical”, and “Complex” we indicate which of these reasoning skills are required to solve the tasks.

V-LoL challenges	Object recognition	Counting	Relational	Spatial	Analogical	Arithmetic	Abstract	Exact Logic
Theory X	✓	✗	✓	✓	✓	✗	✗	✓
Numerical	✓	✓	✓	✓	✗	✓	✓	✓
Complex	✓	✓	✓	✓	✓	✓	✓	✓

- **Arithmetic reasoning** involves reasoning based on numerical information. Therefore, it involves understanding arithmetic operators and comparisons such as ($<$, $>$, \neq , $=$). For example, it is important to understand whether one car has less payloads than another.
- **Analogical reasoning** involves drawing conclusions based on analogous relationships between components of individual objects. In V-LoL, it is required to find analogical relationships in the attributes of the individual cars. E.g. all yellow cars have the same payload.
- **Abstract reasoning** is the ability to draw conclusions based on abstract ideas, concepts, and patterns that are not concretely tied to specific objects (immediately apparent). For example, drawing conclusions by comparing the number of axles with the position of a car or the number of payloads requires abstract reasoning skills.
- **Exact logical reasoning** is the ability to understand and reason based on logical relations which involves understanding and concluding based on logical operators (e.g. \equiv , \wedge , \vee , \neg). Logical reasoning is essential for V-LoL since it involves solving complex reasoning problems that constitute multiple logical operators.

An overview on which class rule (Theory X, Numerical and Complex) addresses which of the visual logical abilities can be found in Tab. 3 showing that each rule allows to investigate a different subset of V-LoL abilities.

B.5 Details on V-LoL Train Semantics

Specifically, the trains of V-LoL consist of a fixed locomotive object pulling a variable number of train cars. Each car is assigned one of five colours: *yellow*, *green*, *grey*, *red*, or *blue*. Moreover, cars exhibit different roof styles, including a empty roof *frame*, a *flat* roof, a *barred* roof, a *peaked* roof, or *no roof* at all. The walls of a car can feature either a *solid* wall or *railings*. Additionally, each car can either be *long* or *short*, equipped with either two or three axles, and capable of carrying a minimum of zero and a maximum of three loads. The available load types include *blue boxes*, *golden vases*, *barrels*, *diamonds*, *metal pots*, and *oval vases*.

B.6 Background Scenes and GT Object Information

Fig. 6 provides an overview of the different possible background scenes and object information provided with each image. On the left we present the four background scenes: base, desert, desert with sky and fisheye scene. On the right we present the ground-truth (GT) information provided with each image. Specifically, for each object we provide a pixel-wise segmentation map, bounding box and an overall depth map.

B.7 Details on Rendering

To render the V-LoL images, we utilize Python 3.10.2 and the Blender Python module version 3.3. The V-LoL 3D representation incorporates the steam locomotive ROCKET by Branislav Kubecka (blenderkit) which is under RF license (This license protects the work in the way that it allows commercial use without mentioning the author, but doesn’t allow for re-sale of the asset in the same form (eg. a 3D model sold as a 3D model or part of assetpack or game level on a marketplace).



Figure 6: Different background scenes and rich scene information provided with each V-LoL sample. The four background options consist of (left): a base, desert, desert with sky, and fisheye scene. The scene information (right) provided with each sample contains: the original image sample, object bounding boxes, pixel-level object segmentation maps and a corresponding depth map.

C Additional experiments

Table 4: Average test accuracy and the respective standard deviation of the neural models trained on different background scenes with varying training set sizes.

ResNet			
	100 images	1000 images	8000 images
Base scene	75,15 ± 3,04	87,32 ± 1,62	99,63 ± 0,14
Desert scene	76,66 ± 1,76	88,58 ± 1,22	99,32 ± 0,19
Sky scene	76,78 ± 3,11	87,86 ± 0,87	98,77 ± 0,71
Fisheye scene	74,21 ± 4,4	85,93 ± 1,34	98,96 ± 0,32
EfficientNet			
	100 images	1000 images	8000 images
Base scene	74,41 ± 3,83	90,43 ± 1,83	99,86 ± 0,08
Desert scene	73,20 ± 1,88	90,14 ± 1,84	99,66 ± 0,12
Sky scene	72,70 ± 2,74	91,45 ± 0,85	99,52 ± 0,15
Fisheye scene	70,36 ± 2,17	88,33 ± 0,91	99,47 ± 0,21
Vision Transformer			
	100 images	1000 images	8000 images
Base scene	63,11 ± 7,28	84,40 ± 2,65	97,17 ± 0,36
Desert scene	62,81 ± 8,24	71,26 ± 4,39	92,40 ± 3,71
Sky scene	60,01 ± 4,29	81,97 ± 2,83	93,03 ± 4,12
Fisheye scene	64,58 ± 3,30	75,88 ± 3,47	92,74 ± 2,39

C.1 Neural performance on the different scenes

In this evaluation we investigate the complexity of different background scenes and renderings on the classification performance of the three neural models, namely ResNet18, where we evaluate the three neural networks on the test sets of each scene. Specifically, we evaluate the models that were trained on different sample sizes of the same background scene. The results can be seen in Tab. 4. We can indeed observe differences in performances across the three models, where on average there is a decrease in accuracies from base, desert, desert with sky to fisheye, with fisheye leading to the lowest

C.2 Out-of-Distribution: Different Attribute Distributions

In this evaluation we investigate the effect of performing inference on V-LoL images with an attribute distribution that is different from that observed during training. Specifically, we investigate the three neural models that were trained on the Michalski attribute distribution, but evaluated on the randomly distributed attributes. The images were generated with the Theory X rule.

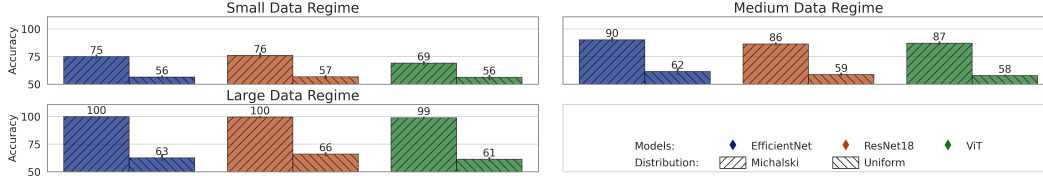


Figure 7: Out-of-Distribution Evaluation. Models were trained on images that were generated with the Michalski attribute distribution and evaluated on two test sets: one also generated via the Michalski distribution and one generated via the random (uniform) attribute distribution. We also provide results here for three training set sizes: 100 (small data regime), 1000 (medium data regime) and 10 000 training images (large data regime).

Fig. 7 presents the results, where we provide the accuracies of the three models that were trained on 100 (small data regime), 1000 (medium data regime) and 10000 images (large data regime) and tested on the test set that was generated with the Michalski attribute distribution as well as on the test set that was generated with the random attribute distribution. We can observe a strong decrease in model performance when evaluated with the out-of-distribution test set. This decrease can be observed in all data size regimes, but becomes even larger the larger the training set size becomes. These results suggest that all three investigated neural models tend to overfit to the training distribution for solving the reasoning tasks.

D Implementation details

For Popper we set the hyperparameters to allow for a maximum of 10 rules each allowing a maximum of 6 variables and 6 literals in its body. Predicate finding and recursion are turned off, as we could not observe any performance improvement. For ALEPH we use the following hyperparameters: $clauselength = 10$, $minacc = 0.6$, $minscore = 3$, $minpos = 3$, $nodes = 5000$, $explore = true$, $max_features = 10$. Both ILP systems are trained and evaluated on the a symbolic ground-truths instead of the visual images.

Our subsymbolic models, namely the ResNet, EfficientNet, and Vision Transformer are initialized with the weights of the pre-trained foundation models which was trained on the 1000-class ImageNet dataset. The last fully-connected layer is replaced to fit the two-class classification task of westbound and eastbound trains. Subsequently, the models are transfer trained on the respective datasets for 25 epochs using a batch size of 50 and starting with a learning rate of 0.001 (0.0001 for the Vision Transformer), which decreases by 20% every five epochs. The Adam optimizer is used for updating the models’ weights and the cross-entropy loss function for calculating the loss.

For the perceptions modules of the Neuro-Symbolic AI systems, we modify the improved mask-RCNN (v2 version) [33] to allow for multi-label instance segmentation. For more in depth implementation details please refer to our code. We initialize our model with pre-trained weights for MaskRCNN + ResNet50 + FPN using the v2 variant with post-paper optimizations. We transfer train our model on 10k V-LoL dataset containing random trains. For training we use the AdamW optimizer and cross-entropy loss. After inferring the segmented masked using mask-RCNN we post process these using a mask matching algorithm to assemble a symbolic scene representations. We achieve nearly 100% validation accuracy on the random V-LoL and 99% test accuracy on the Michalski V-LoL. Subsequently, we fit the ILP approaches using the same hyperparameters as in the run of the purely symbolic AI systems. For beam search of α ILP we choose a beam size of 70 with a beam depth of 5. We select a maximum of 1000 clauses after search on which we then perform learning for 100 epochs. For TheoryX and the numerical rule we learn a logic program consisting of two rules while for the complex rule we learn 4 rules. For more in depth information on the mode declaration and hyper parameters of α ILP, Popper, and Aleph please refer to our code.

All code was run on multiple NVIDIA A100-SXM4-40GB gpus.

E Dataset and Code Availability and License

Access to the data set, data generator and experimental code for reproducing the results are bundled on our website: <https://sites.google.com/view/v-lol>. All data is released under the Creative Commons CC BY 4.0 license. All code is released under the MIT license.

F Dataset Documentation: Datasheets for Datasets

Here we answer the questions outlined in the datasheets for datasets paper by Gebru et al.[19].

F.1 Motivation

For what purpose was the dataset created? V-LoL was created to serve as a challenging benchmark for visual logical learning. By incorporating intricate visual scenes and flexible logical reasoning tasks within a versatile framework, V-LoL provides a platform for investigating a wide range of visual logical learning challenges.

Who created the dataset (e.g., which team, research group) and on behalf of which entity (e.g., company, institution, organisation)? The dataset has been created by the research group “Artificial Intelligence and Machine Learning” at the Computer Science Department, Technical University of Darmstadt.

Who funded the creation of the dataset? The dataset is created for research purposes at AIML. This work was supported by the AI lighthouse project “SPAICER” (01MK20015E), the EU ICT-48 Network of AI Research Excellence Center “TAILOR” (EU Horizon 2020, GA No 952215), and the Collaboration Lab “AI in Construction” (AICO). The work has also benefited from the Hessian Ministry of Higher Education, Research, Science and the Arts (HMWK) cluster projects “The Third Wave of AI” and “The Adaptive Mind”, the Hessian Centre for Artificial Intelligence overall, the Hessian research priority program LOEWE within the project WhiteBox, and from the German Center for Artificial Intelligence (DFKI) project ‘SAINT’.

F.2 Composition

What do the instances that comprise the dataset represent (e.g., documents, photos, people, countries)? The dataset consists of synthetically generated images featuring simulated scenes and segmentation, depth, and metadata detailing scene composition. How many instances are there in total (of each type, if appropriate)? We have generated a total of 11 V-LoL datasets. 8 of which consists 12000 instances respectively, while the remaining 3 are used solely for out-of-distribution (OOD) testing and consist of 2,000 samples each. Does the dataset contain all possible instances or is it a sample (not necessarily random) of instances from a larger set? The datasets represent samples of an infinite set of possible arrangements. One single car sampled from the random distribution has a total of 2200 different permutations. When considering datasets consisting of trains with lengths between 2 and 4, the total number of different car samples is 23.4 trillion. As the number of cars increases, the number of possible samples grows exponentially. For a detailed description of the V-LoL generation process, please refer to Section 3.2.

What data does each instance consist of? Alongside the visually appealing train images, each dataset samples is annotated with detailed scene information including the individual train attributes, object masks, bounding boxes, 3D scene locations, depth information, and symbolically derived ground truth labels.

Is there a label or target associated with each instance? The labels for each instance are symbolically derived from the underlying decision rule of the dataset.

Is any information missing from individual instances? No.

Are relationships between individual instances made explicit (e.g., users’ movie ratings, social network links)? No, there are no relationships between different instances.

Are there recommended data splits (e.g., training, development/validation, testing)? Yes, we split 20% 80% test/train splits for the datasets, with the exception of OOD variant, which is used for evaluation only. We use stratified 5 fold cross-validation.

Are there any errors, sources of noise, or redundancies in the dataset? No.

Is the dataset self-contained, or does it link to or otherwise rely on external resources (e.g., websites, tweets, other datasets)? The dataset is self-contained.

Does the dataset contain data that might be considered confidential (e.g., data that is protected by legal privilege or by doctor-patient confidentiality, data that includes the content of individuals' non-public communications)? No.

Does the dataset contain data that, if viewed directly, might be offensive, insulting, threatening, or might otherwise cause anxiety? No.

Does the dataset relate to people? If not, you may skip the remaining questions in this section. No.

Does the dataset identify any subpopulations (e.g., by age, gender)? NA

Is it possible to identify individuals (i.e., one or more natural persons), either directly or indirectly (i.e., in combination with other data) from the dataset? NA

Does the dataset contain data that might be considered sensitive in any way (e.g., data that reveals racial or ethnic origins, sexual orientations, religious beliefs, political opinions or union memberships, or locations; financial or health data; biometric or genetic data; forms of government identification, such as social security numbers; criminal history)? NA

F.3 Collection Process

How was the data associated with each instance acquired? The data was generated.

What mechanisms or procedures were used to collect the data (e.g., hardware apparatus or sensor, manual human curation, software program, software API)? The images were rendered using Blender 3.3 software on generic systems and Python 3.10.2.

If the dataset is a sample from a larger set, what was the sampling strategy (e.g., deterministic, probabilistic with specific sampling probabilities)? See the similar question in the Composition section.

Who was involved in the data collection process (e.g., students, crowdworkers, contractors) and how were they compensated (e.g., how much were crowdworkers paid)? The authors were involved in the process of generating this dataset.

Over what timeframe was the data collected? The datasets were rendered over a period of several weeks.

Were any ethical review processes conducted (e.g., by an institutional review board)? No.

Does the dataset relate to people? If not, you may skip the remainder of the questions in this section. No.

F.4 Preprocessing/Cleaning/Labeling

Was any preprocessing/cleaning/labeling of the data done (e.g., discretization or bucketing, tokenization, part-of-speech tagging, SIFT feature extraction, removal of instances, processing of missing values)? No, the dataset was generated together with labels.

Was the "raw" data saved in addition to the preprocessed/cleaned/labeled data (e.g., to support unanticipated future uses)? NA

Is the software used to preprocess/clean/label the instances available? NA

F.5 Uses

Has the dataset been used for any tasks already? In the paper we show and benchmark the intended use of this dataset for visual logical learning, specifically evaluating on several challenges of visual logical learning.

Is there a repository that links to any or all papers or systems that use the dataset? No.

What (other) tasks could the dataset be used for? We include additional information maps when generating this dataset, which could be used for object discovery from 3D scenes. In addition the logical structure of the train representations can be converted to natural language questions for QA tasks.

Is there anything about the composition of the dataset or the way it was collected and preprocessed/cleaned/labeled that might impact future uses? No.

Are there tasks for which the dataset should not be used? This dataset is meant for research purposes only.

F.6 Distribution

Will the dataset be distributed to third parties outside of the entity (e.g., company, institution, organization) on behalf of which the dataset was created? No.

How will the dataset will be distributed (e.g., tarball on website, API, GitHub)? The dataset and related evaluation code is available on the website <https://sites.google.com/view/v-lol> allowing users to download and read-in the data.

When will the dataset be distributed? The dataset is available now.

Will the dataset be distributed under a copyright or other intellectual property (IP) license, and/or under applicable terms of use (ToU)? Creative Commons CC BY 4.0 license.

Have any third parties imposed IP-based or other restrictions on the data associated with the instances? The V-LoL 3D representation incorporates the steam locomotive ROCKET by Branislav Kubecka (blenderkit) which is under RF license (This license protects the work in the way that it allows commercial use without mentioning the author, but doesn't allow for re-sale of the asset in the same form (eg. a 3D model sold as a 3D model or part of assetpack or game level on a marketplace). The dataset instances themselves do not have IP-based restrictions.

Do any export controls or other regulatory restrictions apply to the dataset or to individual instances? Not that we are are of.

F.7 Maintenance

Who is supporting/hosting/maintaining the dataset? The dataset is supported by the authors and by the AIML research group.

How can the owner/curator/manager of the dataset be contacted (e.g., email address)? The authors of this dataset can be reached at their e-mail addresses: lukas.henrik.helff@tu-darmstadt.de and wolfgang.stammer@cs.tu-darmstadt.de.

Is there an erratum? If errors are found an erratum will be added to the website.

Will the dataset be updated (e.g., to correct labeling errors, add new instances, delete instances)? Any potential future updates or extension will be communicated via the website. The dataset will be versioned.

If the dataset relates to people, are there applicable limits on the retention of the data associated with the instances (e.g., were individuals in question told that their data would be retained for a fixed period of time and then deleted)? NA

Will older versions of the dataset continue to be supported/hosted/maintained? We plan to continue hosting older versions of the dataset.

If others want to extend/augment/build on/contribute to the dataset, is there a mechanism for them to do so? Yes, we make the dataset generation code available.

F.8 Other Questions

Is your dataset free of biases? Yes.

Can you guarantee compliance to GDPR? No, we are unable to comment on legal issues.

F.9 Author Statement of Responsibility

The authors confirm all responsibility in case of violation of rights and confirm the licence associated with the dataset and its images.